concentrations, some dissociation of R^{II} from C occurred even in the absence of cAMP. To control free cAMP in relatively concentrated (micromolar) solutions of enzyme, we confined the latter inside a microdialysis capillary (150 μm diameter, 9-kD cutoff). The capillary was placed in a solution of intracellular *Aplysia* buffer at high ionic strength (in mM: KOH 250, NaCl 25, $MgCl_2$ 5, glutamate 100, MOPS 300, pH = 7.3) on the stage of the microscope. During its exposure to various [cAMP] outside the capillary, the emission ratios were recorded. The half-maximal ratio change was obtained with 299 ± 53 nM free cAMP (mean ± SE, n = 5). This sensitivity is consistent with estimates in the literature for unlabeled type II kinase [F. Hofmann, J. A. Beavo, P. J. Bechtel, E. G. Krebs, *J. Biol. Chem.* **250**, 7795 (1975)].

8. L. H. P. Botelho, J. D. Rothermel, R. V. Coombs, B. Jastorff, *Methods Enzymol.* **159**, 159 (1988).
9. S. M. Greenberg, L. Bernier, J. H. Schwartz, *J. Neurosci.* **7**, 291 (1987).
10. L. Bernier, V. F. Castellucci, E. R. Kandel, J. H. Schwartz, *ibid.* **2**, 1682 (1982); K. A. Ocorr and J. H. Byrne, *Neurosci. Lett.* **55**, 113 (1985).
11. Values of $D_{[cAMP]}$ of 0.44 × 10^{-5}, 0.97 × 10^{-5}, and 0.33 × 10^{-5} cm^2 s^{-1} have been reported in water [M. Dworkin and K. H. Keller, *J. Biol. Chem.* **252**, 864 (1977)], agar [M. H. Cohen, D. J. Drage, A. Robertson, *Biophys. J.* **15**, 753 (1975)], and molluscan cytoplasm [R. C. Huang and R. Gillette, *J. Gen. Physiol.* **98**, 835 (1991)], respectively.
12. P. J. Bergold *et al.*, *Proc. Natl. Acad. Sci. U.S.A.* **87**, 3788 (1990).
13. The means of pre- and post-stimulus periods (20 to 30 min each) for each cell were compared with the use of an unpaired Student's t test. Translocation was considered significant if $P <$ 0.001 for changes in the ratio of greater than 10%. Experiments with substantial base-line drift were considered uninterpretable and were discarded. We implemented the intensity ratio of fluorescein fluorescence to normalize the potential errors caused by changes in focus, cell shape, illumination intensity, and photobleaching. However, this ratio is not a perfect measure because changes in [cAMP] will artifactually affect the translocation ratio. Although the difference in detectability of C-subunit translocation between single and multiple administrations of serotonin (0 out of 5 and 3 out of 11 cases, respectively) is suggestive, statistical significance is not claimed.
14. N. Dale, S. Schacher, E. R. Kandel, *J. Neurosci.* **7**, 2232 (1987); K. P. Scholz and J. H. Byrne, *Science* **235**, 685 (1987); W. N. Frost, V. F. Castellucci, R. D. Hawkins, E. R. Kandel, *Proc. Natl. Acad. Sci. U.S.A.* **82**, 9266 (1985); P. G. Montarolo *et al.*, *Science* **234**, 1249 (1986).
15. B. Hochner and E. R. Kandel, unpublished data.
16. B.-K. Kaang *et al.*, *Neuron*, in press.
17. D. W. Tank, M. Sugimori, J. A. Connor, R. R. Llinás, *Science* **242**, 773 (1988); R. W. Tsien and R. Y. Tsien, *Annu. Rev. Cell Biol.* **6**, 715 (1990).
18. W. L. Terasaki and G. Brooker, *J. Biol. Chem.* **252**, 1041 (1977); J. S. Hayes and L. L. Brunton, *J. Cyclic Nucleotide Res.* **8**, 1 (1982); J. Barsony and S. J. Marx, *Proc. Natl. Acad. Sci. U.S.A.* **87**, 1188 (1990).
19. B. H. Morimoto and D. E. Koshland, Jr., *Proc. Natl. Acad. Sci. U.S.A.* **88**, 10835 (1991); D. M. Chetkovich, R. Gray, D. Johnston, J. D. Sweatt, *ibid.*, p. 6467; P. Greengard, J. Jen, A. C. Nairn, C. F. Stevens, *Science* **253**, 1135 (1991).
20. S. R. Adams, B. J. Bacskai, S. S. Taylor, R. Y. Tsien, in *Fluorescent Probes for Biological Activity of Living Cells*, W. T. Mason and G. Relf, Eds. (Academic Press, London, 1993), pp. 133–149.
21. R. L. Potter and S. S. Taylor, *J. Biol. Chem.* **254**, 2413 (1979).
22. J. D. Scott *et al.*, *ibid.* **265**, 21561 (1990).
23. The FICRhR was prepared from recombinant C subunits labeled with fluorescein isothiocyanate (*4*) and was combined with type II R subunits labeled with carboxytetramethylrhodamine *N*-hydroxysuccinimidyl ester (*20*). Such R^{II} subunits gave larger fluorescence ratio changes than the previously used R^{I} subunits (*4*). The R^{II} subunits were obtained either by isolation from porcine muscle (*21*) (gift from S. Taylor) or bacterial expression of the murine $R^{II}\alpha$ isoform (*22*) (gift from J. Scott), with similar results.
24. J. Crank, *The Mathematics of Diffusion* (Clarendon, Oxford, 1956).

31 July 1992; accepted 13 January 1993

Increased Frequency of Calcium Waves in *Xenopus laevis* Oocytes That Express a Calcium-ATPase

Patricia Camacho and James D. Lechleiter

When inositol 1,4,5-trisphosphate (IP_3) receptors are activated, calcium is released from intracellular stores in excitatory propagating waves that annihilate each other upon collision. The annihilation phenomenon suggests the presence of an underlying refractory period that controls excitability. Enhanced calcium–adenosine triphosphatase (ATPase) activity might alter the refractory period of calcium release. Expression of messenger RNA encoding the avian calcium-ATPase (SERCA1) in *Xenopus laevis* oocytes increased the frequency of IP_3-induced calcium waves and narrowed the width of individual calcium waves. The effect of SERCA1 expression on calcium wave frequency was dependent on the concentration of IP_3 and was larger at higher (1 μM) than at lower (0.1 μM) concentrations of IP_3. The results demonstrate that calcium pump activity can control IP_3-mediated calcium signaling.

Many hormones and neurotransmitters activate pathways leading to elevations in the intracellular concentration of IP_3 and the subsequent release of Ca^{2+} from intracellular stores (*1*). Cellular signaling information may be encoded in periodic Ca^{2+} oscillations, and much work has focused on defining the underlying basis of these oscillations (*2*). In the spatial domain, Ca^{2+} signaling exhibits a complex variety of patterns. In *Xenopus* oocytes, for example, Ca^{2+} release is initiated at multiple focal sites that generate broken, circular, and spiral waves of Ca^{2+} (*3*, *4*). These observations suggest that the Ca^{2+}-mobilizing machinery acts as an excitable medium (*3*) as it does in other systems such as the classical Belousov-Zhabotinsky reaction, aggregation in the slime mold *Dictyostelium discoideum*, and electrical activity in neuronal and cardiac cells (*5*).

In this theoretical framework of Ca^{2+} signaling, activation of the IP_3 receptor (IP_3R) constitutes the elementary excitatory event (*3*). An important feature of Ca^{2+} release as an excitable medium is the concept of a refractory period, defined as a collection of states in which Ca^{2+} release is inhibited to different degrees, depending on the time elapsed since the preceding wave of excitation (*3*, *6*). Two factors acting singly or in concert may set refractory states of Ca^{2+} release: high cytoplasmic Ca^{2+} concentrations, which inhibit IP_3R activation (*7*), or depletion of Ca^{2+} in the intracellular stores, which inhibits release (*8*). Calcium-ATPases remove Ca^{2+} from the cytoplasm either across the plasma membrane (PMCA family) or into the sarcoplasmic reticulum or endoplasmic reticulum (SERCA family) (*9*). After a Ca^{2+} wave, increased pump activity should reduce cytoplasmic Ca^{2+} concentrations more efficiently and should increase the net uptake of Ca^{2+} into the luminal stores. Increased Ca^{2+}-ATPase expression, however, should not greatly affect the basal concentration of cytosolic Ca^{2+} because in unstimulated cells the Ca^{2+} concentration is too low to activate much pumping activity (*10*).

Oocytes from albino *Xenopus laevis* were injected with SERCA1 mRNA encoding the avian fast twitch Ca^{2+}-ATPase (*11*) and assayed for IP_3-induced Ca^{2+} wave activity 48 to 72 hours later (*12*). To visualize changes in intracellular Ca^{2+}, we injected oocytes with the Ca^{2+} dye indicator Calcium Green I. Individual oocytes were then injected with IP_3 and immediately imaged with confocal microscopy (*13*). A single optical slice near the plasma membrane surface was recorded at 1-s intervals. IP_3 (~1 μM) initiated a wave of Ca^{2+} release across the oocyte (Fig. 1B), which produced an elevated cytoplasmic Ca^{2+} concentration in its wake (*3*, *14*). As the cytoplasmic concentration of Ca^{2+} decreased, pulsatile Ca^{2+} wave activity developed (Fig. 1A). A spatial-temporal stack of 400 consecutive images (Fig. 1C) shows the Ca^{2+} waves generated in response to application of IP_3. In these stacks, time is represented by the z axis (*3*). This oocyte exhibited one of the largest amounts of Ca^{2+} wave activity observed for control oocytes. The average number of Ca^{2+} waves per 400-s temporal stack was 25 ± 14 (mean ± SD, n = 17).

In contrast, the same concentration of

Department of Neuroscience, University of Virginia Health Sciences Center, Charlottesville, VA 22908.

IP_3 (~1 μM) produced markedly different Ca^{2+} wave activity in oocytes that expressed SERCA1 mRNA. First, the initial wave of uniform Ca^{2+} release that envelopes the oocyte was absent (Fig. 1, B and F). Instead, pulsatile Ca^{2+} release occurred immediately after IP_3 injection. Second, the number of Ca^{2+} waves at peak activity was much higher in oocytes that expressed SERCA1 than in control oocytes (Fig. 1, A and E). A similar temporal stack of 400 consecutive images shows the total number of Ca^{2+} waves generated during this period (Fig. 1D). The average number of Ca^{2+} waves per 400-s temporal stack was 64 ± 20 (mean ± SD, n = 17) for oocytes injected with SERCA1 mRNA, 2.6 times that in control oocytes ($P < 0.005$). As another estimate of wave activity, a single 2 × 2 pixel area was monitored for 60 to 120 s during peak Ca^{2+} wave activity (Fig. 1, G and H). This measurement shows the temporal changes of individual Ca^{2+} waves. As observed in the temporal stacks, the average wave period was much longer in control oocytes than in oocytes that expressed SERCA1 (Table 1). Additionally, the width of individual Ca^{2+} waves, estimated as the half-decay time (time required for the peak Ca^{2+} concentration to be reduced by one-half), was shortened in oocytes that expressed SERCA1 transcripts (Table 1). Finally, the IP_3-induced wave activity for both control and SERCA1-expressing oocytes was completely blocked by thapsigargin (1 μM for 1 hour), a specific inhibitor of SERCA-type Ca^{2+}-ATPases (*15*). However, at intermediate concentrations of thapsigargin (100 nM for 1 hour), Ca^{2+} wave activity was decreased but not blocked in four out of five control oocytes. The mean number of Ca^{2+} waves per 400-s temporal stack was 10 ± 9. Thus, as thapsigargin lowers the pumping rate, the frequency of Ca^{2+} waves is correspondingly decreased in comparison to control values.

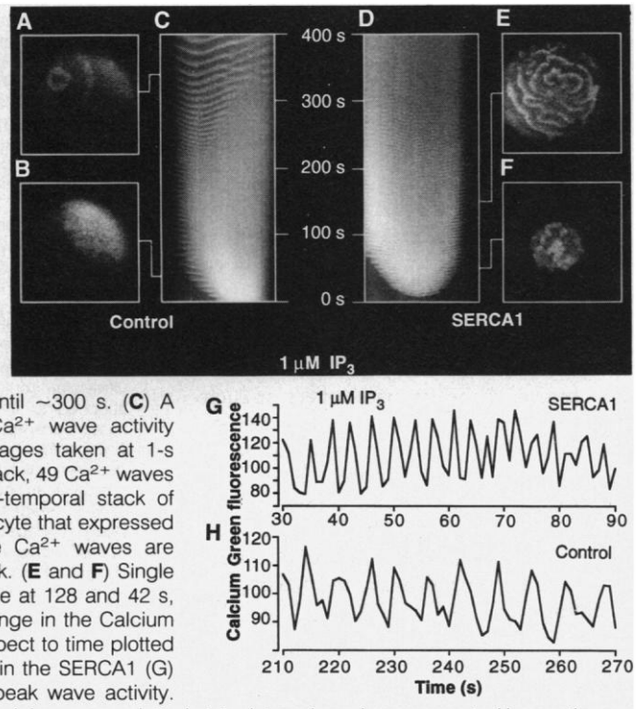

Fig. 1. Spatial temporal patterns of Ca^{2+} release induced by high concentrations of IP_3 (~1 μM) in a control oocyte [(A) through (C)] and in an oocyte injected with SERCA1 mRNA [(D) through (F)]. In (**A**) and (**B**), single optical slices were recorded at 330 and 40 s, respectively. The frequency of pulsatile Ca^{2+} wave activity peaked between 200 and 300 s after injection of IP_3. Regenerative wave activity across the entire oocyte was not observed until ~300 s. (**C**) A spatial-temporal stack of Ca^{2+} wave activity (control) with sequential images taken at 1-s intervals. Within this 400-s stack, 49 Ca^{2+} waves are visible. (**D**) The spatial-temporal stack of Ca^{2+} wave activity for an oocyte that expressed SERCA1 mRNA. Eighty-one Ca^{2+} waves are visible within this 400-s stack. (**E** and **F**) Single optical slices of Ca^{2+} release at 128 and 42 s, respectively. (**G** and **H**) Change in the Calcium Green fluorescence with respect to time plotted for a fixed 2 × 2 pixel area in the SERCA1 (G) and control (H) images at peak wave activity. Individual data points from each image are plotted at 1-s intervals and are connected by continuous line segments.

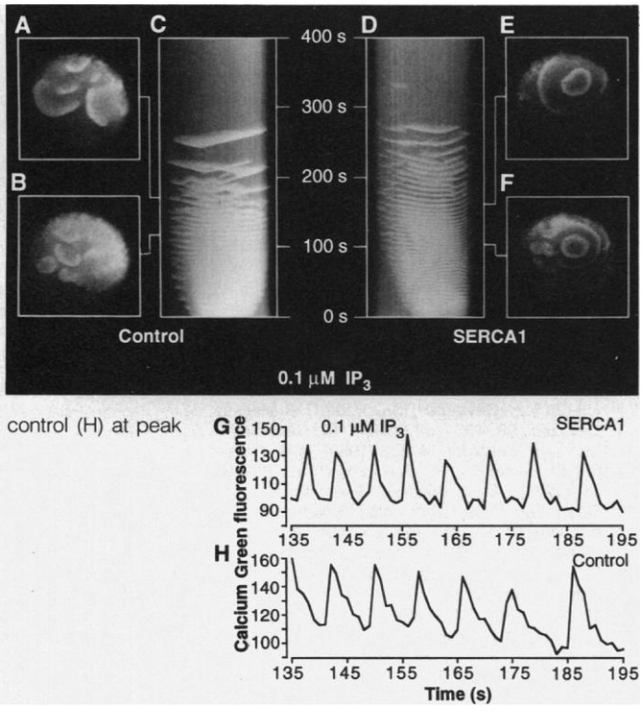

Fig. 2. Comparison of Ca^{2+} wave activity induced by low concentrations of IP_3 (~0.1 μM) in a control (**A** through **C**) or SERCA1-expressing (**D** through **F**) oocyte. Single optical slices were recorded 170 s (A), 118 s (B), 161 s (E), and 102 s (F) after application of IP_3. In (C) and (D) are shown temporal stacks (400 s) of Ca^{2+} wave activity for the control and SERCA1-expressing oocytes, respectively. (**G** and **H**) Temporal graphs for SERCA1 (G) and control (H) at peak Ca^{2+} wave activity.

At low concentrations of IP_3, the frequency of Ca^{2+} waves was lower and the length of time during which Ca^{2+} waves were observed was also shortened. However, even at lower IP_3 concentrations, the greatest amount of Ca^{2+} wave activity was still observed in oocytes that expressed SERCA1 Ca^{2+}-ATPase (Fig. 2). In control oocytes, IP_3 initially induced a large Ca^{2+} wave, which left cytoplasmic Ca^{2+} temporarily elevated (Fig. 2B); pulsatile wave activity developed only after 20 to 30 s (Fig. 2, A through C). In oocytes that expressed SERCA1, pulsatile wave activity was immediately induced by IP_3 injection (Fig. 2, D through F). The increased pumping activity was observed as a narrowing in the width of single Ca^{2+} waves, as seen in individual confocal images (Fig. 2, A and E) and in the intensity plots from a single oocyte location (Fig. 2, G and H). Table 1 shows a comparison of the characteristics of waves induced by high and low concentrations of IP_3.

Because the frequency of Ca^{2+} oscillations has been correlated with ligand concentrations (*2*, *16*), we also examined the effects of low concentrations of IP_3 (~0.1 μM) on Ca^{2+} wave activity both in control oocytes and oocytes that expressed SERCA1. At low concentrations of IP_3,

A monoclonal antibody (mAb) to the avian Ca^{2+} pump (*17*) reacted with a single band at ~100 kD in immunoblots of membrane-bound proteins prepared from oocytes injected with mRNA (Fig. 3A). Control oocytes did not react with the SERCA1

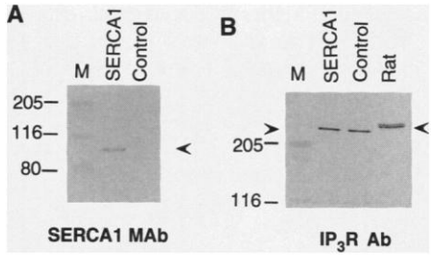

Fig. 3. Protein immunoblot analysis of SERCA1 and the IP_3R in *Xenopus* oocytes. (**A**) A single protein band (arrowhead) was recognized by a mAb to SERCA1 in oocytes injected with SERCA1 mRNA. The antibody did not recognize an endogenous SERCA1 product in control oocytes injected with water. An equal amount of protein (10 μg) was loaded in each lane. M, prestained molecular size standards (Bio-Rad, Melville, New York). (**B**) A polyclonal antibody to the IP_3R recognized a single band in oocytes injected with either water or SERCA1 mRNA (left arrowhead). The same IP_3R antibody recognized a doublet (right arrowhead) in membrane extracts prepared from rat brain (*18*). Markers (M) are as in (A) but run on a 4% gel. Molecular size markers are indicated to the left of (A) and (B) in kilodaltons.

Table 1. Calcium wave parameters at peak activity with treatment with 1 μM or 0.1 μM IP_3. The wave period, half-decay time, and velocity were first averaged for each oocyte during peak wave activity. Each number represents the mean ± SD of these individual oocyte averages.

Oocyte (*n*)	Wave period (s)	Half-decay time (s)	Velocity (μm/s)
	1 μM IP_3		
SERCA1 (5)	3.9 ± 0.4	1.0 ± 0.2	21.1 ± 2.7
Control (6)	7.9 ± 0.6	1.8 ± 0.1	19.5 ± 4.6
	0.1 μM IP_3		
SERCA1 (5)	7.9 ± 0.9	1.6 ± 0.2	20.0 ± 3.0
Control (5)	10.2 ± 2.5	2.4 ± 0.6	21.4 ± 1.4

mAb. To exclude the possibility that the amount of IP_3R was increased by overexpression of the SERCA1 Ca^{2+}-ATPase, we measured the amount of the IP_3R with a polyclonal antibody to the rabbit IP_3R in immunoblots of the same protein fractions (*18*). The amount of IP_3R did not change in SERCA1-expressing oocytes (Fig. 3B). The endogenous IP_3R product from the oocyte appears as a single band of smaller molecular size (~256 kD) than that from rodent brain (which migrates characteristically as a doublet at ~260 to 273 kD and is shown as a positive control) (*19*). These data suggest that the enhanced frequency of Ca^{2+} waves is a result of the enhanced Ca^{2+}-ATPase activity and not a change in the number of IP_3Rs.

Calcium pump activity has been associated primarily with Ca^{2+} homeostasis (*20*). The frequency modulation of Ca^{2+} waves by SERCA1 expression points toward an expanded role for Ca^{2+}-ATPases in Ca^{2+} signaling. The concentration of Ca^{2+} is important in the regulation of IP_3-induced Ca^{2+} release. At low concentrations, Ca^{2+} acts as agonist with IP_3, whereas at high concentrations Ca^{2+} inhibits IP_3R channel activity (*7*). Calcium release may also be inhibited indirectly by depletion of the Ca^{2+} stores (*8*, *21*). SERCA1 activity is likely to modulate the frequency of IP_3-induced Ca^{2+} wave activity by controlling one of these Ca^{2+}-dependent mechanisms of inhibition. In terms of an excitable medium, increased pumping shortens the refractory period for Ca^{2+} release. This effect should be most apparent at wave frequencies where activity is normally so high that consecutive waves impinge on areas that are refractory because a preceding wave has recently passed through them (*6*). In agreement with this, SERCA1 expression produced the strongest effect at high IP_3 concentrations where Ca^{2+} waves propagated in closer proximity without wave velocity being affected (Table 1). Because Ca^{2+}-ATPase activity and expression are known to be regulated (*22*), our data suggest Ca^{2+} pump modulation may be a critical factor in controlling IP_3-mediated Ca^{2+} signaling.

REFERENCES AND NOTES

1. M. J. Berridge and R. F. Irvine, *Nature* **341**, 197 (1989); R. W. Tsien and R. Y. Tsien, *Annu. Rev. Cell Biol.* **6**, 715 (1990); C. W. Taylor and A. Richardson, *Pharmacol. Ther.* **51**, 97 (1991); C. D. Ferris and S. H. Snyder, *Annu. Rev. Physiol.* **54**, 469 (1992); M. J. Berridge, *Nature* **361**, 315 (1993).
2. P. E. Rapp and M. J. Berridge, *J. Exp. Biol.* **93**, 119 (1981); N. M. Woods, K. S. R. Cuthbertson, P. H. Cobbold, *Nature* **319**, 600 (1986); M. J. Berridge, *Cell Calcium* **12**, 63 (1991); L. F. Jaffe, *Proc. Natl. Acad. Sci. U.S.A.* **88**, 9883 (1991); T. Meyer and L. Stryer, *Annu. Rev. Biophys. Chem.* **20**, 153 (1991).
3. J. Lechleiter, S. Girard, D. Clapham, E. Peralta, *Nature* **350**, 505 (1991); J. Lechleiter, S. Girard, E. Peralta, D. Clapham, *Science* **252**, 123 (1991); J. D. Lechleiter and D. E. Clapham, *Cell* **69**, 283 (1992; I. Parker and Y. Yao, *Proc. R. Soc. London Ser. B* **246**, 269 (1991).
4. S. DeLisle and M. J. Welsch, *J. Biol. Chem.* **267**, 7963 (1992).
5. A. N. Zaikin and A. M. Zhabotinsky, *Nature* **225**, 535 (1970); A. T. Winfree, *Science* **175**, 634 (1972); P. N. Devreotes, M. J. Potel, S. A. Mackay, *Dev. Biol.* **96**, 405 (1983); N. A. Goroleva and J. Bures, *J. Neurobiol.* **14**, 353 (1983); M. A. Allesie, F. I. M. Bonke, F. J. G. Schopman, *Circ. Res.* **33**, 54 (1973); A. T. Winfree, *When Time Breaks Down: The Three-Dimensional Dynamics of Electrochemical Waves and Cardiac Arrhythmias* (Princeton Univ. Press, Princeton, NJ, 1987).
6. R. N. Miller and J. Rinzel, *Biophys. J.* **34**, 227 (1981); J. D. Dockery, J. P. Keener, J. J. Tyson, *Physica D* **30**, 177 (1988).
7. M. Iino, *J. Gen. Physiol.* **95**, 1103 (1990); I. Parker and I. Ivorra, *Proc. Natl. Acad. Sci. U.S.A.* **87**, 260 (1990); E. A. Finch, T. J. Turner, S. M. Goldin, *Science* **252**, 443 (1991); I. Bezprozvanny, J. Watras, B. E. Ehrlich, *Nature* **351**, 751 (1991); M. Iino and M. Endo, *ibid.* **360**, 76 (1992).
8. A. Goldbeter, G. Dupont, M. J. Berridge, *Proc. Natl. Acad. Sci. U.S.A.* **87**, 1461 (1990); L. Missiaen, C. W. Taylor, M. J. Berridge, *Nature* **352**, 241 (1991).
9. E. Carafoli, *Annu. Rev. Physiol.* **53**, 531 (1991); A. K. Grover and I. Khan, *Cell Calcium* **13**, 9 (1992).
10. J. Lytton, M. Westlin, S. E. Burk, G. E. Shull, D. H. MacLennan, *J. Biol. Chem.* **267**, 14483 (1992).
11. A. M. Campbell, P. D. Kessler, Y. Sagara, G. Inesi, D. M. Fambrough, *ibid.* **266**, 16050 (1991).
12. Capped [$m^7G(5')ppp(5')G$; Pharmacia, Piscataway, NJ] synthetic transcripts of SERCA1 were generated from plasmid pCMV-SERCA1 linearized with Xba I and transcribed with T7 RNA polymerase (BRL, Grand Island, NY). The transcripts were resuspended in water at a concentration of 2 μg/μl. Two to 3 days before the experiment, defolliculated oocytes were injected with a bolus of 50 nl of synthetic mRNA encoding SERCA1 or with an equal volume of water (control oocytes).
13. Oocytes were injected with a solution of Calcium Green I (50 nl, 250 μM) 30 to 60 min before each experiment (~12.5 μM final concentration, assuming a 1:20 dilution). Calcium Green I (Molecular Probes, Eugene, OR) was prepared in Ca^{2+}-free water with Polymetal Sponge (Molecular Probes). Images (170 × 170 pixels) were acquired at 1-s intervals with a Bio-Rad MRC 600 ultraviolet confocal laser–scanning microscope attached to a Nikon Diaphot with a ×10 (0.5 numerical aperture) UVfluor Nikon objective lens. The confocal aperture was set at the largest opening, which produced a 868 by 868 by 32 μm optical slice, and the photomultiplier gain was set at 6.5. Images were analyzed with ANALYZE (Mayo Foundation, Rochester, MN) on a Sun Sparc2 workstation. Images were not filtered for analysis or display. Calcium increases are reported in arbitrary intensity units because of the inherent inaccuracies in calibrating non-ratioing dyes [A. B. Harkins, N. Kurebayashi, S. Hollingworth, S. M. Baylor, *Biophys. J.* **59**, 240 (1991)]. An in vivo calibration with Ca^{2+} buffer kit II (Molecular Probes) placed resting concentrations between 50 to 100 nM, with peak Ca^{2+} concentrations >300 nM. We induced calcium wave activity by injecting a bolus of 50 nl of IP_3 (Calbiochem, La Jolla, CA) of either 20 μM (~1 μM final concentration, assuming 1:20 dilution) or 2 μM (~0.1 μM final) stock solutions. All recordings were made in the absence of extracellular Ca^{2+} [96 mM NaCl, 2 mM KCl, 2 mM $MgCl_2$, 5 mM Hepes (pH 7.5) (Gibco), and 1 mM EGTA (Sigma)].
14. W. B. Busa, J. E. Ferguson, S. K. Joseph, J. R. Williamson, R. Nuccitelli, *J. Cell Biol.* **101**, 677 (1985).
15. O. Thastrup, P. J. Cullen, B. K. Drobak, *Proc. Natl. Acad. Sci. U.S.A.* **87**, 2466 (1990).
16. S. DeLisle, K. Krause, G. Denning, B. V. L. Potter, M. J. Welsh, *J. Biol. Chem.* **265**, 11726 (1990).
17. N. J. Karin, Z. Kaprielian, D. M. Fambrough, *Mol. Cell. Biol.* **9**, 1978 (1989).
18. Extracts enriched in endoplasmic reticulum were prepared from pools of four to ten oocytes that were rinsed in ice-cold phosphate-buffered saline and resuspended in ice-cold lysis buffer (10 to 20 μl per oocyte) [20 mM tris (pH 7.5), 2 mM EDTA, 0.5 mM EGTA, 5 mM β-mercaptoethanol, 2 mM phenylmethylsulfonyl fluoride, and leupeptin (0.01 mg/ml)]. After homogenization and centrifugation at 10,000*g* for 15 s, the supernatant was collected and the sedimented material was again homogenized and centrifuged. The two supernatants were combined and centrifuged at 100,000*g* for 1 hour. To isolate the membrane-bound proteins, we resuspended the sedimented material in lysis buffer that contained 1% NP-40 (Pierce, Rockford, IL) and centrifuged it at 10,000*g* for 15 min. The supernatant, which contained the membrane-bound protein fraction, was acetone-precipitated and resuspended in 1% SDS. The protein content was determined spectrophotometrically with the bicinchoninic acid protein assay (Pierce). Oocyte

extracts (10 μg) were separated by SDS–polyacrylamide gel electrophoresis (8% gel for the SERCA1 immunoblot and 4% gel for the IP_3R blot). After electrophoresis, the proteins were transferred to nitrocellulose. The avian SERCA1 immunoblot was probed with a mAb extract (mouse antibody to chicken) diluted 1:1500. The IP_3R immunoblot was probed with a polyclonal antibody (rabbit antibody to mouse) diluted 1:2000. The IP_3R immunoblot is negative when incubated with preimmune serum (P. Camacho and J. D. Lechleiter, unpublished data). After incubation with primary antibody, exposure to a secondary alkaline phosphatase (AP)–conjugated immunoglobulin G (IgG) was done according to the manufacturer's instructions (goat antibody to mouse IgG for SERCA1 and goat antibody to rabbit IgG for the IP_3R, both from Promega, Madison, WI). Colorimetric detection was obtained within 20 min of exposure to the NET/BCIP color substrates (ProtoBlot protein immunoblot AP system, Promega).

19. G. A. Mignery, T. C. Südhof, K. Takei, P. De Camilli, *Nature* **342**, 192 (1989); T. Furuichi *et al.*, *ibid.*, p. 32; J. B. Parys *et al.*, *J. Biol. Chem.* **267**, 18776 (1992).
20. E. Carafoli, *Annu. Rev. Biochem.* **56**, 395 (1987).
21. S. Girard, A. Luckhoff, J. Lechleiter, J. Sneyd, D. Clapham, *Biophys. J.* **61**, 509 (1992).
22. C. Brandl, N. Green, B. Korczak, D. H. MacLennan, *Cell* **44**, 597 (1986); C. Brandl, S. deLeon, D. Martin, D. H. MacLennan, *J. Biol. Chem.* **262**, 3768 (1987); A. Gunteski-Hamblin, J. Greeb, J. Shull, *ibid.* **263**, 15032 (1988); J. Lytton and D. H. MacLennan, *ibid.*, p. 15024.

23. We thank K. Takeyasu for the avian SERCA1 cDNA and mAb, P. DeCamilli for the polyclonal antibody to the IP_3R, D. Castle for rat brain membrane extracts, and H. Kutchai, E. Nasi, and E. Peralta for their critical reading of the manuscript.

3 November 1992; accepted 12 January 1993

Acceleration of Intracellular Calcium Waves in *Xenopus* Oocytes by Calcium Influx

Steven Girard and David Clapham*

Many cell membrane receptors stimulate the phosphoinositide (PI) cycle, which produces complex intracellular calcium signals that regulate diverse processes such as secretion and transcription. A major messenger of this cycle, inositol 1,4,5-trisphosphate (IP_3), stimulates its receptor channel on the endoplasmic reticulum to release calcium into the cytosol. Activation of the PI cycle also induces calcium influx, which refills the intracellular calcium stores. Confocal microscopy was used to show that receptor-activated calcium influx, enhanced by hyperpolarization, modulates the frequency and velocity of IP_3-dependent calcium waves in *Xenopus laevis* oocytes. These results demonstrate that transmembrane voltage and calcium influx pathways may regulate spatial and temporal patterns of IP_3-dependent calcium release.

Propagating waves of elevated intracellular Ca^{2+} may be triggered in *Xenopus* oocytes by the activation of muscarinic receptors or by the microinjection of either guanosine-5′-O-(3-triphosphate) or IP_3 isomers (*1–4*). Calcium release from IP_3-sensitive intracellular stores (*5*) is necessary for both initiation and propagation of these waves (*2–4*). IP_3-dependent Ca^{2+} waves persist in the oocyte for up to 30 min in the absence of extracellular Ca^{2+} (*2, 3*). We used confocal fluorescence microscopy with conventional two-electrode voltage clamp to study Ca^{2+} influx and its influence on IP_3-dependent Ca^{2+} waves (*6–9*). Fluorescence from Calcium Green was recorded from superficial optical sections (628 by 419 μm) within ~30 μm of the plasma membrane (*10*).

To investigate the effects of Ca^{2+} influx on receptor-induced Ca^{2+} transients, we applied acetylcholine (ACh) to oocytes that expressed human m3 muscarinic acetylcholine receptors (m3AChRs) (Fig. 1). Saturating concentrations of ACh (50 μM) triggered Ca^{2+} release from intracellular stores, which resulted in an increased concentration of Ca^{2+} that slowly decayed to base line over ~10 min (Fig. 1, A to D) (*11*). Hyperpolarization in the presence of 2.5 mM extracellular Ca^{2+} induced Ca^{2+} influx up to ~13 min after the application of atropine (200 μM) (*12*). In contrast to the generalized Ca^{2+} transient induced by high concentrations of ACh, submaximal stimulation (0.2 to 1 μM ACh) triggered regenerative Ca^{2+} waves (Fig. 1, E to G) that appear as streaks of increased fluorescence in a volume projection (Fig. 1F). The Ca^{2+} waves and Ca^{2+}-activated Cl^- current ($I_{Cl,Ca}$) oscillations stopped within seconds after the application of atropine (200 μM at 550 s), whereas the hyperpolarization-induced influx of extracellular Ca^{2+} persisted for more than 7 min (Fig. 1F) (*13*). Unstimulated cells showed no Ca^{2+} influx with hyperpolarization ($n = 5$). Because Ca^{2+} influx persisted for minutes after the Ca^{2+} waves were abolished, we speculate that other second messenger mechanisms triggered Ca^{2+} entry or that the concentrations of IP_3 were sufficient to bind to a receptor site that caused Ca^{2+} influx (*14*). These results also show that Ca^{2+} influx caused a generalized increase in Ca^{2+} but did not itself cause regenerative waves.

We examined the influence of Ca^{2+} influx on Ca^{2+} waves induced by injection of a nonmetabolizable IP_3 analog, inositol 1,4,5-trisphosphorothioate (IP_3S_3) (*15*). In the absence of extracellular Ca^{2+}, the waves induced by IP_3S_3 (5 μM) had a period, or interval between transients, that slowly increased over time (Fig. 2, A to D). The Ca^{2+} wave velocity was independent of membrane potential in ten experiments conducted in the absence of extracellular Ca^{2+} (Fig. 2E), which indicates that the kinetics of the IP_3 receptor (IP_3R) channel are not directly altered by changes in membrane potential.

In the presence of 2.5 mM extracellular Ca^{2+}, hyperpolarization triggered Ca^{2+} influx in 35 of 46 oocytes injected with IP_3S_3 (5 μM) (*16*), and no Ca^{2+} influx was observed in noninjected oocytes under similar conditions ($n = 10$). The entry of extracellular Ca^{2+} reversibly affected the frequency and velocity of Ca^{2+} waves triggered by IP_3S_3 (5 μM) (Fig. 3), an effect that was blocked by extracellular La^{3+} (1 mM) (*17*). In one oocyte, the wave velocity varied with the holding potential after the concentration of extracellular Ca^{2+} was raised to 2.5 mM (Fig. 3D). The mean velocity increased from 25.1 ± 0.8 μm s^{-1} ($n = 5$) to 33 ± 2 μm s^{-1} ($n = 3$) during a second hyperpolarizing pulse from −15 to −70 mV with 2.5 mM extracellular Ca^{2+}, and after depolarization to −15 mV the velocity returned to 25.4 ± 0.9 μm s^{-1} ($n = 2$). The wave velocity in this experiment ranged from 19 to 37 μm s^{-1} and was correlated with the local base line fluorescence before each wave (Fig. 3F). These data suggest that the influx of extracellular Ca^{2+} may alter the propagation of IP_3-dependent Ca^{2+} waves by increasing the basal Ca^{2+} concentration. This modulation of the velocity of Ca^{2+} waves was best observed with large changes in the membrane potential (~70 mV), which correlate to larger Ca^{2+} influxes.

Depolarization, which reduces the driving force for Ca^{2+} entry into the cell, decreased the resting concentration of Ca^{2+} and increased the period between successive wave fronts (Fig. 4, A to H). These alterations in wave frequency were reversible (Fig. 1, E and F, and Figs. 3 and 4). Calcium Green signals from 33-μm square regions (Fig. 4A) showed that the frequency of Ca^{2+} waves increased from 1.8 ± 0.2 min^{-1} at 0 mV to 5.2 ± 1.4 min^{-1} at −50 mV (mean ± SEM; $n = 9$). A comparison of the local Calcium Green signal from one region (Fig. 4G) and the signal averaged over the entire slice (Fig. 4H) showed that averaging over the entire section obscures the high frequency waves. Regions capable of initiating waves at −50 mV but not at more depolarized potentials appear as short segments of fluorescence in the volume projection (Fig. 4E), which suggests that different regions have unique threshold cytosolic Ca^{2+} concentrations that must be reached before waves are initiated. This

Department of Pharmacology, Mayo Foundation, Rochester, MN 55905.

*To whom correspondence should be addressed.